

Fluctuations of flow harmonics in Pb+Pb collisions at $\sqrt{s_{NN}} = 2.76$ TeV from the Glauber model*

MACIEJ RYBCZYŃSKI¹ AND WOJCIECH BRONIEWSKI^{1,2}

¹Institute of Physics, Jan Kochanowski University, PL-25406 Kielce, Poland

²The H. Niewodniczański Institute of Nuclear Physics, Polish Academy of Sciences, PL-31342 Kraków, Poland

In the framework of the Glauber model as implemented in `GLISSANDO 2`, we study the fluctuations of flow harmonics in Pb+Pb collisions at the LHC energy of $\sqrt{s_{NN}} = 2.76$ TeV. The model with wounded nucleons and the admixture of binary collisions leads to reasonable agreement for the ellipticity and triangularity fluctuations with the experimental data from the ATLAS, ALICE, and CMS collaborations, verifying the assumption that the initial eccentricity is approximately proportional to the harmonic flow of charged particles. While the agreement, in particular at the level of event-by-event distributions of eccentricities/flow coefficients is not perfect, it leads to a fair (at the level of a few percent for all centralities except the most peripheral collisions) description of the scaled standard deviation and the F measure which involves the four-particle cumulants. We also discuss the case of quadrangular flow. Computer scripts that generate our results from the `GLISSANDO 2` simulations are provided.

PACS numbers: 25.75.-q

1. Introduction

Studies of correlations and fluctuations are in the core of the heavy-ion physics program, as they carry valuable information on the dynamics of the system in the early and intermediate stages of the collision. In particular, the azimuthal angle distributions of the produced hadrons have been a subject of extensive experimental studies at RHIC (see, e.g., [1, 2, 3] and more recently at the LHC [4, 5, 6, 7, 8]).

In this paper we present predictions of the Glauber model of the initial stage of the heavy-ion reactions for fluctuations of the flow harmonics.

* e-mails: Maciej.Rybczynski@ujk.edu.pl, Wojciech.Broniowski@ifj.edu.pl

While many such studies have been presented in the literature (see, e.g., the references in the recent review in Ref. [9], or the latest works [10, 11, 12, 13, 14, 15]), recently some confusion has been raised by results published in Ref. [6, 7] claiming, that the Glauber model fails badly for the fluctuations of flow (cf. Figs. 13-14 from Ref. [7] and Fig. 18 from Ref. [6]). In this paper we show, that this is not the case, and that the agreement with the experimental results of Refs. [4, 7, 8] holds at the expected level for a wide range of centralities. While the agreement is not perfect for the event-by-event distributions of eccentricities/flow coefficients, showing differences in the tails of these distributions, the global measures, such as the event-by-event standard deviation or the F measures, are reproduced at a level of a few percent for all centralities except the most peripheral collisions. So the basic outcome of our work is that the Glauber model works for the description of the fluctuations of ellipticity and triangularity. It also works, for a somewhat lesser accuracy, for the quadrangular flow.

The consistency of the Glauber model with the data is important, as the approach is used as one of the baselines of the early-stage modeling in numerous analyses, also the experimental ones, where the connection of centrality to the number of participants is made with the help of Glauber simulations. We provide computer scripts that generate our results from the GLISSANDO 2 [16, 17] simulations if the reader wishes to effortlessly repeat or extend our results.

The formalism used in this paper is described in detail in Ref. [18]. In particular, all details concerning the statistical methods and the popular variants of the Glauber models may be found there, so in this paper we limit the presentation to the minimum.

2. Glauber model

We use GLISSANDO 2 [16, 17] to analyze two variants of the Glauber model with Monte Carlo simulations:

1. The *mixed* model, amending wounded nucleons [19] with an admixture of binary collisions [20, 21, 22, 23] in the proportion α . The successful fits to particle multiplicities (see Ref. [23]) give $\alpha = 0.145$ at $\sqrt{s_{NN}} = 200$ GeV. For the LHC energy of $\sqrt{s_{NN}} = 2.76$ TeV we take $\alpha = 0.15$.
2. Each source from the mixed model may deposit entropy with a certain distribution of strength. Therefore, we superpose the Gamma distribution over the distribution of sources and label this model. The choice of this distribution follow from the fact that when folded with the Poisson distribution for the production of the number of particles at freeze-out, it yields the popular negative binomial distribution.

The expression for the initial entropy distribution in the transverse plane is

$$s(\mathbf{x}_T) = \text{const} \left(\frac{1 - \alpha}{2} \sum_{i=1}^{N_w} w_i g_i(\mathbf{x}_T) + \alpha \sum_{j=1}^{N_{\text{bin}}} w_j g_j(\mathbf{x}_T) \right), \quad (1)$$

where

$$g_k(\mathbf{x}_T) = \exp \left(-\frac{(\mathbf{x}_T - \mathbf{x}_{T,k})^2}{2\sigma^2} \right) \quad (2)$$

describes the smearing of the sources (wounded nucleons or binary collisions) located at $\mathbf{x}_{T,k}$. The smearing parameter is $\sigma = 0.4$ fm [24]. The center of the binary-collision source is at the mean of the location of the centers of the colliding nucleons.

The choice of weights w_k requires a careful discussion. In our approach [25] there are two sources of fluctuations: in the early stage, stemming from the statistical nature of the collision process, and in the final stage, from statistical hadronization. When we are interested in the initial shape, we should include only fluctuations generated at this stage. With no weight fluctuations here we simply set $w_i = 1$, and with the Gamma fluctuations included, w_i are generated randomly from the Gamma distribution [16].

When we are interested in the multiplicity fluctuations (as in Sec. 3), we look at the system in the final phase, therefore we need to overlay the Poisson distribution from the statistical hadronization. Then w_i is generated from the Poisson distribution in the model with no weight fluctuations in the Glauber phase, and from the negative binomial distribution in the model with Gamma fluctuations in that phase.

3. Multiplicity fluctuations in p+Pb collisions

The need for the overlaid distribution comes from the physical fact that the individual collisions deposit fluctuating amount of energy in the transverse plane. Moreover, such fluctuations are necessary to reproduce the particle spectrum at very large multiplicities. One may use the multiplicity distribution measured in the p+Pb collisions [26] to adjust the parameters of the negative binomial distribution

$$N_{\lambda,\kappa}(n) = \frac{\Gamma(n + \kappa) \lambda^n \kappa^\kappa}{\Gamma(\kappa) n! (\lambda + \kappa)^{n+\kappa}}, \quad (3)$$

where the multiplicity n ($= w_\kappa$) has the mean $\langle n \rangle = \lambda$ and variance $\sigma(n)^2 = \lambda(1 + \lambda/\kappa)$. With $\lambda = 9.3$ and $\sigma(n) = 10.3$ we obtain the matching displayed

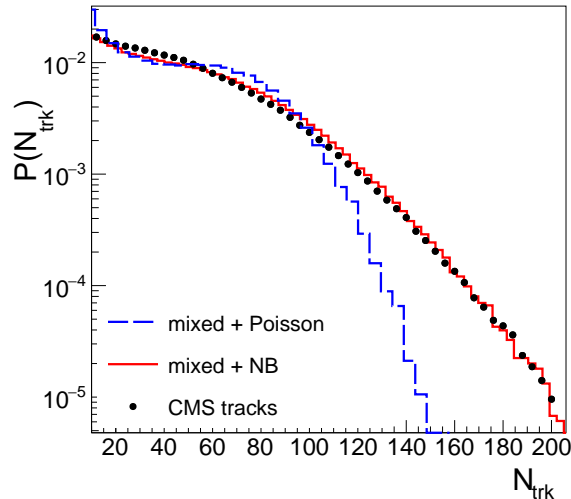


Fig. 1. Multiplicity distribution in p+Pb collisions, where the CMS data [26] are for charged tracks with $p_T > 0.4$ GeV and $|\eta| < 2.4$, and the lines denote GLISSANDO 2 results for the mixed+Poisson (dashed line) and mixed+NB (solid line) models. We note that the weight fluctuations in the Glauber phase (generated with the Gamma distribution) are essential for the agreement of the high-multiplicity tail.

in Fig. 1, where we compare the model result to the CMS data [26]. On the other hand, the model without the weight fluctuation in the early phase (labeled *mixed+Poisson*) in Fig. 1 fails to reproduce the data.

That way we fix the parameters of the overlaid distribution. Correspondingly, in the analysis of the eccentricities in the next sections we use value of $\nu = 0.9$ in the Gamma distribution

$$g(w, \nu) = \frac{w^{\nu-1} \nu^\nu \exp(-\nu w)}{\Gamma(\nu)}, \quad w \in [0, \infty). \quad (4)$$

which yields $\langle w \rangle = 1$ and $\sigma(w) = 1/\sqrt{\nu} = 1.054$.

The realistic nucleon-nucleon inelastic collision profile for the LHC energies is taken from Ref. [27]. We use an excluded distance $d = 0.9$ fm when generating the nucleon configurations in the nuclei. In the case of *mixed+ Γ* variant we use the correlated configurations of nucleons in Pb nuclei provided by [28]. The total inelastic nucleon-nucleon cross section is equal to 64 mb for the investigated Pb+Pb collisions at $\sqrt{s_{NN}} = 2.76$ TeV.

4. Fluctuations of elliptic and triangular flow

Due to collectivity of the fireball evolution, the azimuthal anisotropy of hadrons produced in the final state reflects the initial spatial asymmetry of the fireball in the transverse plane, which is due to geometry [29] and event-by-event fluctuations [30, 31, 32, 33, 34, 35]. The observed particle distributions are characterized by the harmonic flow coefficients v_n , defined as the Fourier coefficients of the expansion

$$\frac{dN}{d\phi} = \frac{N}{2\pi} \left[1 + 2 \sum_{n=2}^{\infty} v_n \cos [n(\phi - \Psi_n)] \right]. \quad (5)$$

(in this paper we use the v_n coefficients integrated over the transverse momentum for symmetric systems and at mid-rapidity).

Analogously, the eccentricity coefficients ϵ_n parametrize the shape of the initial fireball, and are defined in a given event as

$$\epsilon_n e^{in\Phi_n} = \frac{\int dx_T s(\mathbf{x}_T) \rho^n e^{in\phi}}{\int dx_T s(\mathbf{x}_T) \rho^n}, \quad (6)$$

where ρ and ϕ are the polar coordinates corresponding to \mathbf{x}_T , and the source density $s(\mathbf{x}_T)$ is given in Eq. (1). The event-plane angles Ψ_n and Φ_n are interesting in their own right [36, 37], but are not important for the analysis shown in this paper.

It has been argued (see, e.g., Ref. [11, 12, 14, 38]) that to a good accuracy one has the proportionality (the ‘‘shape-flow’’ transmutation)

$$v_n = \kappa_n \epsilon_n, \quad n = 2, 3, \quad (7)$$

where the constants κ_n depend on features of the colliding system (centrality selection, mass numbers, collision energy) and the properties of the dynamics (viscosity of quark-gluon plasma, initial time of collective evolution, freeze-out conditions). Yet, when the above-mentioned conditions are fixed, Eq. (7) holds to sufficient accuracy that allows for model-independent predictions. Technically, Eq. (7) means that the response of the system to small shape deformation, for a given class on initial conditions such as centrality selection, is linear. The feature is limited to $n = 2, 3$, as for higher harmonics nonlinear effects may be substantial [39].

From Eq. (7) one obtains immediately the relation for the scaled (i.e., independent of the mean) quantities

$$\frac{v_n}{\langle v_n \rangle} = \frac{\epsilon_n}{\langle \epsilon_n \rangle}, \quad n = 2, 3, \quad (8)$$

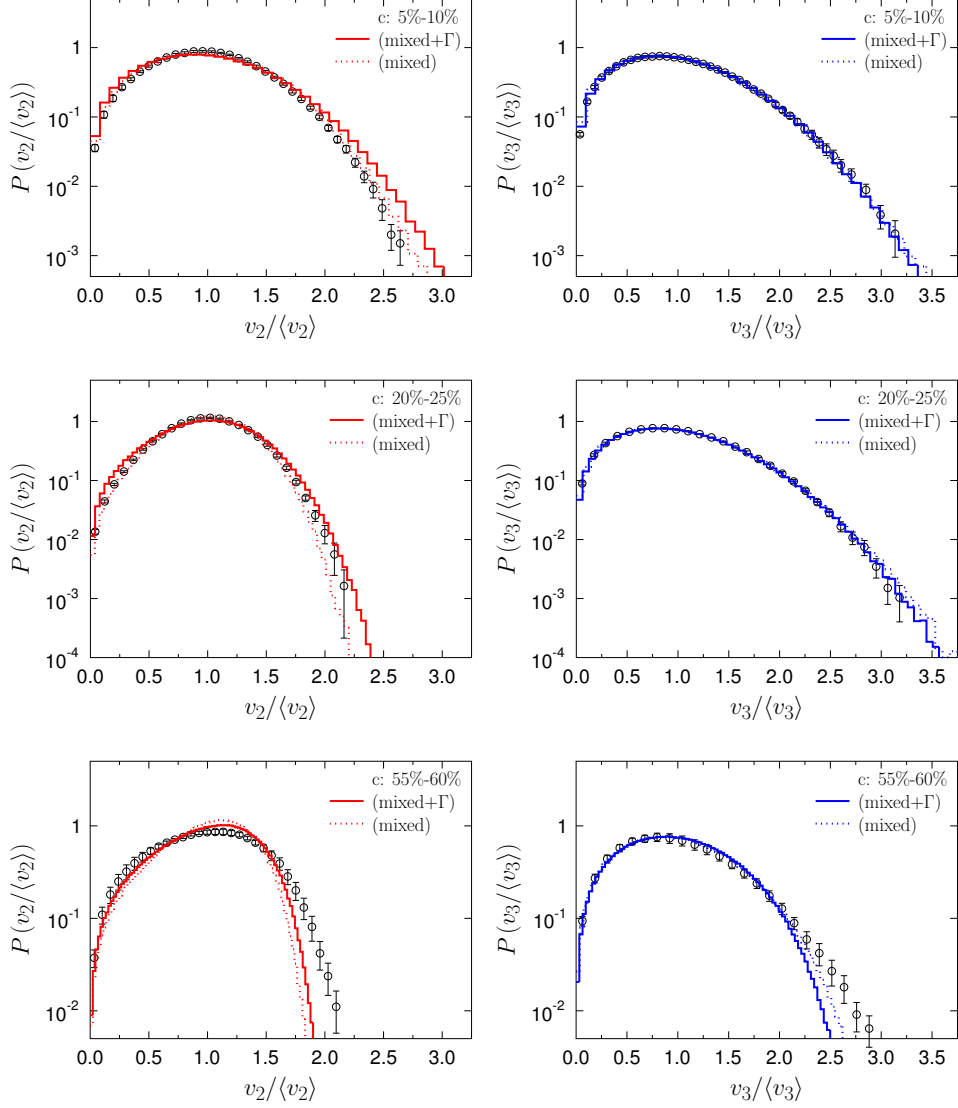


Fig. 2. Distributions of $\epsilon_n/\langle\epsilon_n\rangle$ for the model calculations, compared to the experimental distribution of $v_n/\langle v_n\rangle$ from the ATLAS collaboration [6]. Top row: centrality 5 – 10%, middle row: centrality 20 – 25%, bottom row: centrality 55 – 60%.

where $\langle.\rangle$ denotes averaging over events in the given class. Equation (8) means that the event-by-event distributions of the scaled quantities should

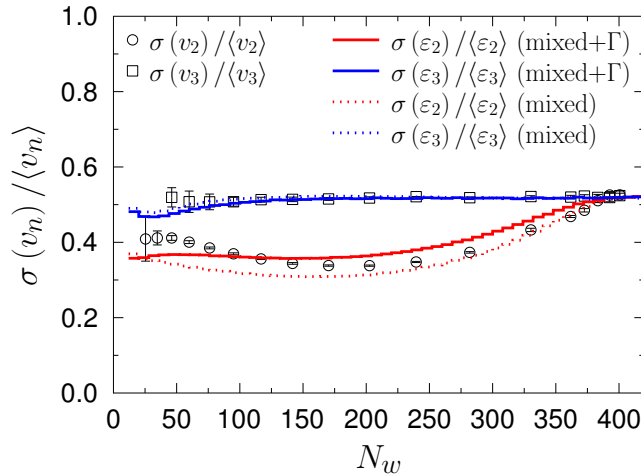


Fig. 3. The scaled event-by-event standard deviation for the eccentricities, $\sigma(\epsilon_n)/\langle\epsilon_n\rangle$, and for the harmonic flow coefficients $\sigma(v_n)/\langle v_n\rangle$, plotted as functions of the number of wounded nucleons N_w . The dashed (solid) lines correspond to our simulation in the mixed (mixed+ Γ). The data come from the ATLAS [6] collaboration.

be equal, i.e., $p(v_n/\langle v_n\rangle) = p(\epsilon_n/\langle\epsilon_n\rangle)$. As seen from Fig. 2, this is indeed the case to expected accuracy. The agreement with the ATLAS data is not perfect, especially for the ellipticity case, where the model distribution is somewhat too wide for the most central events and too narrow for the most peripheral events. This agrees qualitatively with the results of Refs. [13, 14].

With the approximate equality of the distributions for the scaled quantities, the same feature holds for various statistical moments. Below, we explore the two-particle and four-particle cumulants moments [40], defined as

$$\begin{aligned}\epsilon_n\{2\} &= \langle\epsilon_n^2\rangle^{1/2}, \\ \epsilon_n\{4\} &= 2(\langle\epsilon_n^2\rangle^2 - \langle\epsilon_n^4\rangle)^{1/4}.\end{aligned}\tag{9}$$

More specifically, we take the scaled event-by-event standard deviation, $\sigma(\epsilon_n)/\langle\epsilon_n\rangle$, and the $F_n(\epsilon_n)$ moments defined as

$$F(\epsilon_n) = \sqrt{\frac{\epsilon_n\{2\}^2 - \epsilon_n\{4\}^2}{\epsilon_n\{2\}^2 + \epsilon_n\{4\}^2}}.\tag{10}$$

These measures are analogously defined for the flow coefficients v_n . Accord-

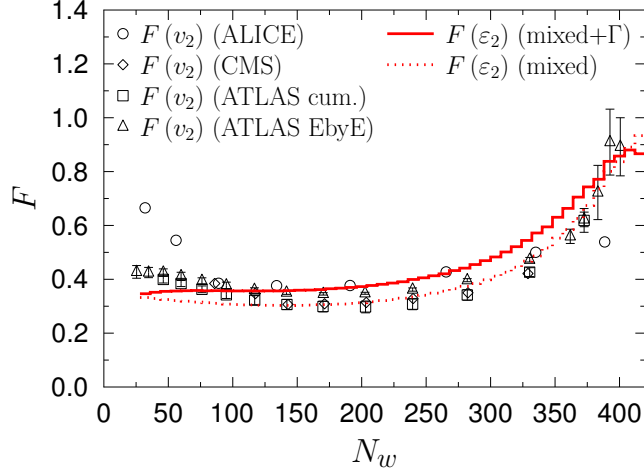


Fig. 4. The relative elliptic flow event-by-event fluctuations measure $F(v_2)$, plotted as a function of the number of wounded nucleons N_w . Result of our simulation with the mixed+ Γ model is displayed with the solid line, whereas the dashed line shows the outcome of the mixed model. The points show the data from ATLAS [7], ALICE [4], and CMS [8] collaborations.

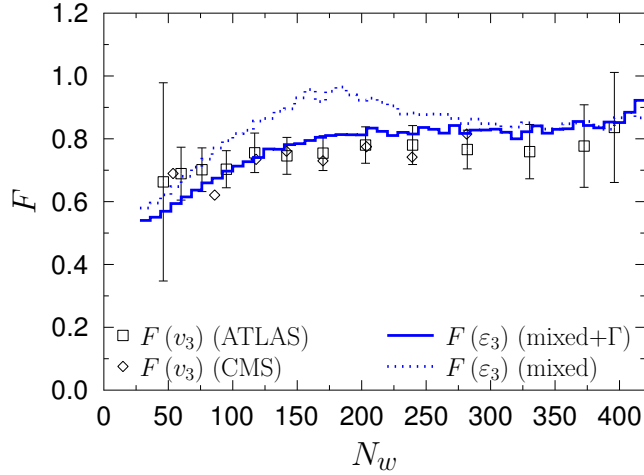


Fig. 5. Same as in Fig. 4 but for $F(v_3)$.

ing to what has been said, one expects the approximate relations

$$\frac{\sigma(\epsilon_n)}{\langle \epsilon_n \rangle} \simeq \frac{\sigma(v_n)}{\langle v_n \rangle}, \quad n = 2, 3 \quad (11)$$

and

$$F(\epsilon_n) \simeq F(v_n), \quad n = 2, 3. \quad (12)$$

The comparison with the recent LHC data is made in Figs. 3-5, where we plot the scaled standard deviation and the F_n as functions of the number of wounded nucleons N_w . We note a very reasonable agreement for sufficiently central collisions ($N_w > 100$). These results should be juxtaposed to Figs. 13-14 of Ref. [7] or Fig. 18 from Ref. [6], which show that these papers report incorrect results from the Glauber simulations. We note that for the most central events, where only fluctuations contribute to eccentricities, we have $\sigma(\epsilon_n)/\langle\epsilon_n\rangle \rightarrow \sqrt{4/\pi - 1}$ [18], and $F(\epsilon_n) \rightarrow 1$. For peripheral collisions ($N_w < 100$) the agreement is poorer, calling for improvement.

5. Quadrangular flow

The above analysis was carried out for $n = 2$ and $n = 3$, as it has been claimed in the literature that higher rank flow coefficients are more complicated due to non-linear effects, incorporating for instance the ϵ_2^2 contributions in v_4 , etc. [39]. Nevertheless, we have tested that taking the relation (7) also for the case $n = 4$, i.e. $v_4 = \kappa\epsilon_4$, leads to very reasonable behavior of the flow fluctuations. The results are shown in Fig. 6, which are fine for central and semi-central events. On the other hand, taking the strong nonlinear response $v_4 = \kappa\epsilon_2^2$ would lead to substantial disagreement, with $\sigma(\epsilon_2)/\langle\epsilon_2\rangle \rightarrow 1$, high above the data for $\sigma(v_4)/\langle v_4\rangle$. We note that a small nonlinear admixture in v_4 is not excluded, but the bulk contribution should come from just the linear response to ϵ_4 , as suggested by Fig. 6.

6. Conclusions

Our main results are as follows:

1. Glauber model works within expected accuracy for the flow measures $\sigma(\epsilon_n)/\langle\epsilon_n\rangle$ and $F(v_n)$, for $n = 2, 3$, but also for $n = 4$.
2. Our results for ellipticity and triangularity fluctuations agree qualitatively with the studies of Ref. [11, 13, 14], but correct the results of the Glauber simulations presented in Refs. [6, 7].
3. Our results for the investigated measures do not depend strongly on the details of the Glauber model (overlaid distribution, correlations in the nuclear distributions, wounding profile, etc.), hence are robust for the investigation of flow fluctuations.

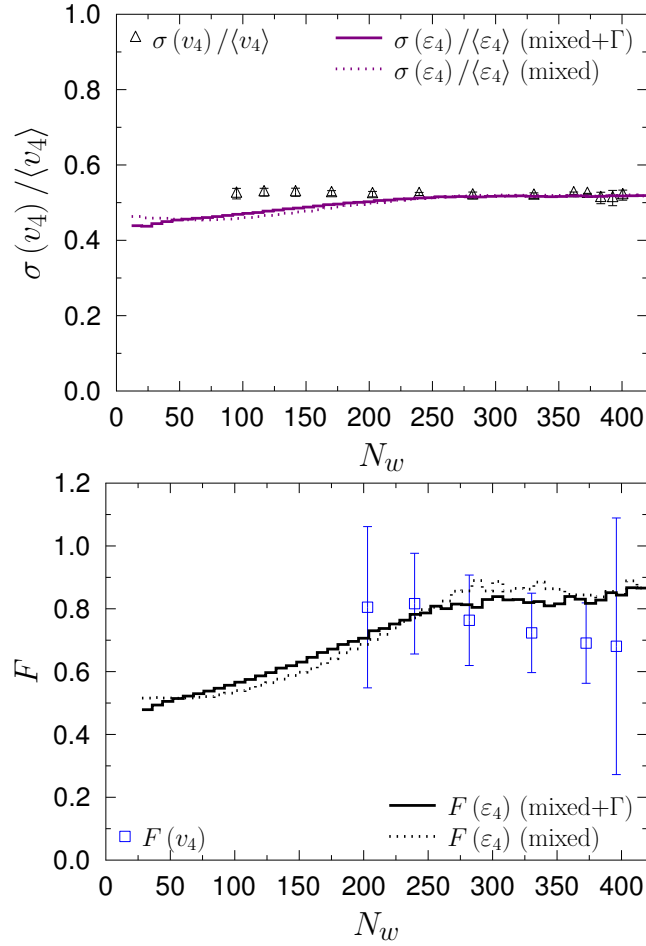


Fig. 6. The measures $\sigma(\epsilon_4)/\langle \epsilon_4 \rangle$ (top panel) and $F(v_4)$ (bottom panel), compared to the ATLAS data [6] for the corresponding quantities for the quadrangular flow coefficient v_4 .

We thank Piotr Bożek for a helpful discussion. Research supported by the National Science Center grants DEC-2012/05/B/ST2/02528 and DEC-2012/06/A/ST2/00390.

Appendix A

Running the simulations

To reproduce the results of the simulations presented in this paper, or to extend them to other physical cases, the user should download the package **GLISSANDO 2** ver. 2.9 [17] from the web page

<http://www.ujk.edu.pl/homepages/mryb/GLISSANDO/>

and after unpacking execute (on UNIX systems) the following commands:

```
make
./glissando2 input/mixed_gamma.dat output/mixed_gamma_01.root
root -b -l -q -x "macro/eps_fluct.C(\"output/mixed_gamma\",1)"
```

More statistics can be accumulated by running, for instance

```
./glissando2 input/mixed_gamma.dat output/mixed_gamma_02.root
...
./glissando2 input/mixed_gamma.dat output/mixed_gamma_10.root
root -b -l -q -x "macro/eps_fluct.C(\"output/mixed_gamma\",10)"
```

The plots are placed in the **output** directory. The present code has been checked with **ROOT** ver. 5.34.

REFERENCES

- [1] STAR, P. Sorensen, J. Phys. G34 (2007) S897, nucl-ex/0612021.
- [2] PHOBOS, B. Alver, Int. J. Mod. Phys. E16 (2007) 3331.
- [3] PHOBOS, B. Alver et al., J. Phys. G34 (2007) S907, nucl-ex/0701049.
- [4] ALICE Collaboration, K. Aamodt et al., Phys. Rev. Lett. 105 (2010) 252302, 1011.3914.
- [5] ALICE, B. Abelev et al., Phys. Lett. B719 (2013) 18, 1205.5761.
- [6] ATLAS Collaboration, G. Aad et al., JHEP 1311 (2013) 183, 1305.2942.
- [7] ATLAS, G. Aad et al., Eur. Phys. J. C74 (2014) 3157, 1408.4342.
- [8] CMS, S. Chatrchyan et al., Phys. Rev. C89 (2014) 044906, 1310.8651.
- [9] M. Luzum and H. Petersen, J. Phys. G41 (2014) 063102, 1312.5503.
- [10] Z. Qiu and U.W. Heinz, Phys. Rev. C84 (2011) 024911, 1104.0650.
- [11] H. Niemi et al., Phys. Rev. C87 (2013) 054901, 1212.1008.
- [12] A. Bzdak, P. Bożek and L. McLerran, Nucl.Phys. A927 (2014) 15, 1311.7325.
- [13] T. Renk and H. Niemi, Phys. Rev. C89 (2014) 064907, 1401.2069.
- [14] J. Fu, Phys. Rev. C92 (2015) 024904.
- [15] L.V. Bravina et al., (2015), 1509.02692.
- [16] W. Broniowski, M. Rybczyński and P. Bożek, Comput. Phys. Commun. 180 (2009) 69, 0710.5731.

- [17] M. Rybczyński et al., *Comput. Phys. Commun.* 185 (2014) 1759, 1310.5475.
- [18] W. Broniowski, P. Bożek and M. Rybczyński, *Phys. Rev. C* 76 (2007) 054905, 0706.4266.
- [19] A. Białas, M. Bleszyński and W. Czyż, *Nucl. Phys.* B111 (1976) 461.
- [20] D. Kharzeev and M. Nardi, *Phys. Lett.* B507 (2001) 121, nucl-th/0012025.
- [21] J. Schaffner-Bielich et al., *Nucl. Phys.* A705 (2002) 494, nucl-th/0108048.
- [22] PHOBOS, B.B. Back et al., *Phys. Rev. C* 65 (2002) 031901, nucl-ex/0105011.
- [23] PHOBOS, B.B. Back et al., *Phys. Rev. C* 70 (2004) 021902, nucl-ex/0405027.
- [24] P. Bożek and W. Broniowski, *Phys. Rev. C* 88 (2013) 014903, 1304.3044.
- [25] A. Olszewski and W. Broniowski, *Phys.Rev. C* 88 (2013) 044913, 1303.5280.
- [26] CMS, S. Chatrchyan et al., CMSPublic Web (2012), <http://twiki.cern.ch/twiki/bin/view/CMSPublic/PhysicsResultsHIN12015>.
- [27] M. Rybczyński and Z. Włodarczyk, *J.Phys.* G41 (2013) 015106, 1307.0636.
- [28] M. Alvioli, H.J. Drescher and M. Strikman, *Phys. Lett.* B680 (2009) 225, 0905.2670.
- [29] J.Y. Ollitrault, *Phys. Rev. D* 46 (1992) 229.
- [30] PHOBOS Collaboration, B. Alver et al., *Phys. Rev. Lett.* 98 (2007) 242302, nucl-ex/0610037.
- [31] S.A. Voloshin, (2006), nucl-th/0606022.
- [32] Y. Hama et al., *Phys.Atom.Nucl.* 71 (2008) 1558, 0711.4544.
- [33] B. Alver and G. Roland, *Phys. Rev. C* 81 (2010) 054905, 1003.0194.
- [34] M. Luzum, *J.Phys.* G38 (2011) 124026, 1107.0592.
- [35] R.S. Bhalerao, J.Y. Ollitrault and S. Pal, *Phys. Lett.* B742 (2015) 94, 1411.5160.
- [36] P. Bożek and W. Broniowski, (2015), 1506.02817.
- [37] P. Bożek, W. Broniowski and J. Moreira, *Phys. Rev. C* 83 (2011) 034911, 1011.3354.
- [38] P. Bożek et al., *Phys.Rev. C* 90 (2014) 064902, 1410.7434.
- [39] D. Teaney and L. Yan, *Phys. Rev. C* 83 (2011) 064904, 1010.1876.
- [40] N. Borghini, P.M. Dinh and J.Y. Ollitrault, *Phys. Rev. C* 63 (2001) 054906, nucl-th/0007063.